Standardization phantom for intra-operative fluorescence molecular imaging

Dimitris Gorpas[a,b], Maria Anastasopoulou[a,b], Maximilian Koch[a,b], Uwe Klemm[a], Markus Nieberler[c], Vasilis Ntziachristos[a,b]

[a]Helmholtz Zentrum München, Institute for Biological and Medical Imaging, Ingolstädter Landstrasse 1, Neuherberg D-85764, Germany; [b]Technical University Munich, Chair for Biological Imaging, Arcisstrasse 21, Munich D-80333, Germany; [c]Technical University Munich, Department of Oral and Maxillofacial Surgery, University Hospital rechts der Isar, Arcisstrasse 21, Munich D-80333, Germany

ABSTRACT

Fluorescence-guided intervention is increasingly considered for real-time intra-operative oncological applications. Herein we propose a novel composite phantom for standardization and quality control, which could serve as a framework toward good clinical practices.

Keywords: Fluorescence molecular imaging; composite phantom; standardization; benchmarking; data referencing

1. INTRODUCTION

Fluorescence molecular imaging is increasingly considered for intra-operative oncological applications, such as cancer detection at earlier stages [1] or surgical guidance and decision-making assistance by more accurate delineation of tumor margins [2, 3]. Currently several clinical studies are implemented to assess novel fluorescence agents with sensitivity and specificity to moieties upregulated by cancer, while a number of different targeted fluorescence agents have been granted approval for experimental use in humans [2].

The exciting and never-before seen outcomes of these studies have naturally promoted several developments in fluorescence molecular imaging systems. However, the variety of technology implementations and operational characteristics has led to the paradox the studies carried out with markedly different systems cannot be compared, even if the fluorescence tracer is the same [4, 5].

Therefore, methods for standardizing fluorescence imaging is an unmet need for assessing the performance of various systems and agents and for providing a reference to the recorded data [4]. During the last few years there has been proposed a number of phantoms targeting the comparison and/or validation of fluorescence imaging systems [6, 7]. Most of these phantoms, however, resolve one or a few parameters and provide a limited characterization of the variables associated with fluorescence imaging performance.

In current work, we demonstrate a composite solid phantom that facilitates multiple targets within the field of view of the imaging system and thus allows for the characterization of a relatively large number of performance parameters [8]. Namely these parameters include sensitivity as a function of optical properties and depth, resolution (optical and fluorescence/diffused), cross-talk, and illumination homogeneity. Furthermore, data analysis is implemented automatically and no specialized training is required for image capturing, and data analysis and interpretation [9]. This demonstrates the exciting potential of this phantom for clinical translation and its application as calibration and benchmarking target.

2. MATERIALS AND METHODS

2.1 Phantom

A schematic of the developed phantom is shown in Fig. 1a. The base material was transparent polyurethane (WC-783 A/B, BJB Enterprises, Tustin, United States). To enable fluorescence imaging at the near-infrared regime organic

*v.ntziachristos@tum.de; phone: +49(0)8931873852;

quantum dots (Qdot ® 800 ITK™, Q21771MP, Thermofisher Scientific Waltham, United States) were employed, while scattering and absorption were imposed by anatase TiO 2 nanoparticles (Titanium IV Oxide, Sigma Aldrich, St. Louis, United States) and Hemin (Sigma Aldrich, from bovine ≥90%) correspondingly. Alcohol soluble nigrosin (Sigma Aldrich) was used to mimick absorption at the phantom matrix, instead of Hemin. The photostability of the phantom materials has been the major factor for their selection [6]. A United States Air Force (USAF-1951) test chart was attached to the phantom for estimating the optical resolution of the imaging system.

2.2 Data processing

Following image acquisition, automated extraction of all phantom components was implemented through application of the speeded-up robust features (SURF) algorithm. Two templates were designed, one for the fluorescence images of the phantom and one for the reflectance images (i.e. in case of hybrid fluorescence/color imaging systems). The application of the SURF algorithm provides the geometric transformation to project the template onto the acquired images, and thus enables the extraction of all phantom components. This allows for the quantification of the camera performance metrics, i.e., magnification, optical resolution, diffused fluorescence resolution, excitation light leakage and parasitic illumination, sensitivity, dynamic range, and field illumination homogeneity, without any user interference. All metrics were quantified by means of: (1) signal-to-noise ratio (SNR), and (2) contrast [9].

To demonstrate the use of the phantom we employed a hybrid fluorescence/color imaging system previously developed by our group [10].

3. RESULTS

Figure 1b shows the acquired fluorescence (left) and color (right) phantom images, following the application of the SURF-based segmentation algorithm. All boundaries have been colored according to the scheme adopted in Fig. 1a. Given that the segmentation is referred to a template, translation of the fluorescence image to the color image coordinates, and vice versa, is enabled without additional registration procedures. This is appreciated in Fig. 1c. Following segmentation, correction for illumination inhomogeneity is performed in the color image. As seen in Fig. 1d, vignetting is addressed, with degradation to image quality or color.

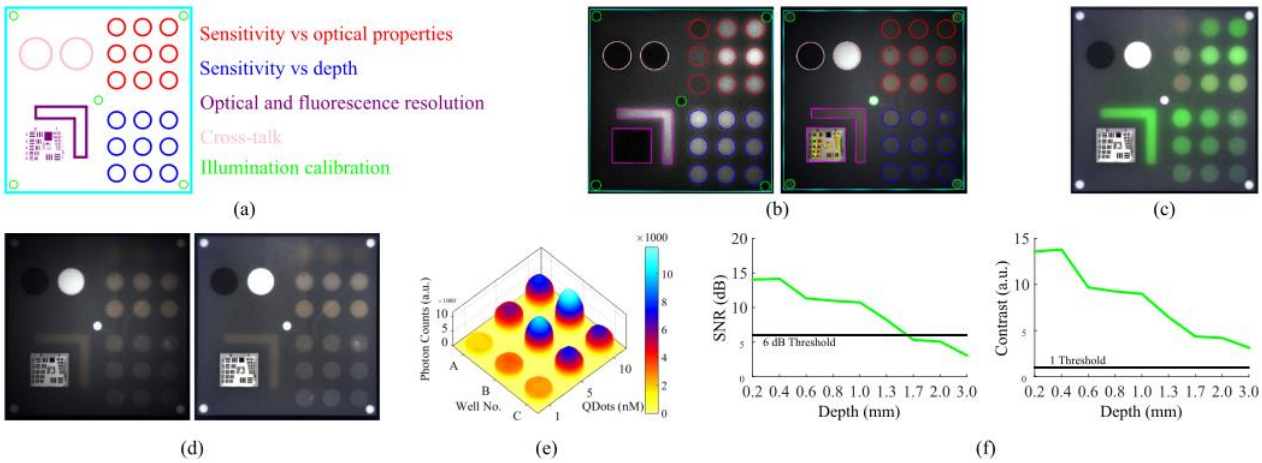

Fig. 1. **Standardization phantom and its application**. **(a)** A schematic of the phantom with all targets color coded. **(b)** Segmented fluorescence (left) and color (right) images acquired from the phantom. Borders have been color-coded according to (a). **(c)** Overlay of phantom fluorescence image onto the corresponding color one, as acquired by the hybrid fluorescence molecular imaging system. **(d)** Field illumination calibration removes the vignetting present in the raw color image (left) without degrading its quality or color (right). **(e)** Photon counts from the area targeting sensitivity vs optical properties. **(f)** SNR and contrast from the area targeting sensitivity vs depth. Any well showing value below the corresponding thresholds is assumed not detectable.

All performance parameters can then be quantified and visualized. Fig. 1e shows the per pixel photon counts of the phantom area assessing sensitivity versus different optical properties, while Fig. 1f illustrates SNR and contrast of the area assessing sensitivity versus depth. All this information can be employed to characterize a fluorescence molecular imaging system, as well to compare it with others of markedly different specifications. Additionally, the interpretation of

these data is straightforward and comprehensive. For example, the SNR threshold for assuming a detectable target is 6 dB. This means, in Fig. 1f, every phantom well with SNR below this threshold is not detectable by the camera. Comparison of such metrics derived by different systems leads to system benchmarking.

4. CONCLUSION

The study presented herein present a composite solid phantom and its application for fluorescence molecular imaging systems characterization. Such phantom has the potential to be employed for system benchmarking, a challenge needed to be address for a successful clinical translation of this very promising imaging technology. The phantom, relying on noncontact measurements and without need of specialized training, can immediately be translated into clinical environments and used for referencing and calibration of existing systems.

ACKNOWLEDGMENT

This work was funded by the Deutsche Forschungsgemeinschaft (DFG), Germany [Gottfried WilhelmLeibniz Prize 2013; NT 3/10-1].

REFERENCES

[1] Nagengast W. B., Hartmans E., Garcia-Allende P. B., Peters F. T. M., Linssen M. D., Koch M., Koller M., Tjalma J. J. J., Karrenbeld A., Jorritsma-Smit A., Kleibeuker J. H., van Dam G. M., and Ntziachristos V., "Near-infrared fluorescence molecular endoscopy detects dysplastic oesophageal lesions using topical and systemic tracer of vascular endothelial growth factor a," Gut **68**(1), 7-10 (2019).

[2] Koch M., and Ntziachristos V., "Advancing surgical vision with fluorescence imaging," Annu Rev Med **67**(1), 153-164 (2016).

[3] Dsouza A. V., Lin H., Henderson E. R., Samkoe K. S., and Pogue B. W., "Review of fluorescence guided surgery systems: Identification of key performance capabilities beyond indocyanine green imaging," J Biomed Opt **21**(8), 080901 (2016).

[4] Koch M., Symvoulidis P., and Ntziachristos V., "Tackling standardization in fluorescence molecular imaging," Nat Photonics **12**(9), 505-515 (2018).

[5] Pogue B. W., Zhu T. C., Ntziachristos V., Paulsen K. D., Wilson B. C., Pfefer J., Nordstrom R. J., Litorja M., Wabnitz H., Chen Y., Gioux S., Tromberg B. J., and Yodh A. G., "Fluorescence-guided surgery and intervention — an aapm emerging technology blue paper," Med Phys **45**(6), 2681-2688 (2018).

[6] Zhu B., Tan I. C., Rasmussen J. C., and Sevick-Muraca E. M., "Validating the sensitivity and performance of near-infrared fluorescence imaging and tomography devices using a novel solid phantom and measurement approach," Technol. Cancer. Res. Treat. **11**(1), 95-104 (2012).

[7] Pogue B. W., and Patterson M. S., "Review of tissue simulating phantoms for optical spectroscopy, imaging and dosimetry," J. Biomed. Opt. **11**(4), 041102 (2006).

[8] Anastasopoulou M., Koch M., Gorpas D., Karlas A., Klemm U., Garcia-Allende P. B., and Ntziachristos V., "Comprehensive phantom for interventional fluorescence molecular imaging," J. Biomed. Opt. **21**(9), 091309 (2016).

[9] Gorpas D., Koch M., Anastasopoulou M., Klemm U., and Ntziachristos V., "Benchmarking of fluorescence cameras through the use of a composite phantom," J Biomed Opt **22**(1), 016009 (2017).

[10] van Dam G. M., Themelis G., Crane L. M. A., Harlaar N. J., Pleijhuis R. G., Kelder W., Sarantopoulos A., de Jong J. S., Arts H. J. G., van der Zee A. G. J., Bart J., Low P. S., and Ntziachristos V., "Intraoperative tumor-specific fluorescence imaging in ovarian cancer by folate receptor-[alpha] targeting: First in-human results," Nat. Med. **17**(10), 1315-1319 (2011).